Monte Carlo simulations of the effect of shielding on H retention in the Moon's surface and the H_2 exosphere.

O. J. Tucker and W. M. Farrell NASA Goddard Space Flight Center 8800 Greenbelt Rd., MD 20771

Introduction: Infrared spectra of the Moon's surface obtained by the Moon Mineralogy Mapper (M^3) provide evidence for a global OH veneer. M^3 observations indicate the surface concentration varies with latitude, time of day, surface composition and when shielded in the Earth's magnetotail [1]. Recently, we modeled M^3 surface densities presented in Li and Milliken (2017) [1] using a Monte Carlo simulation. The model linked the M^3 observations of hydrogen within the surface to LAMP observations of the H_2 exosphere. The model highlighted the effect hindered H diffusion due to the formation of metastable OH on the surface degassing rates [2]. Here we used this model including the effect of shielding by Earth's magnetosphere on both the H surface content and H_2 exosphere for qualitative comparisons to M^3 observations [3].

Background: Throughout most of the Moon's 29.5 day orbit its surface is exposed to the unperturbed solar wind which is primarily composed of protons with a density of $n_{sw} = 5 \times 10^6$ H^+/m^3 at flow speeds of v_{sw} = 400 km/s. However, for 6 – 8 days of the orbit when the Moon traverses Earth's magnetosheath and magnetotail its surface is partially shielded from the solar wind yet still exposed to the terrestrial plasma environment. ARTEMIS (Acceleration, Reconnection, Turbulence, and Electrodynamics of the Moon's Interaction with the Sun) measurements indicate the proton flux incident on the Moon's surface on average can be reduced by approximately an order of magnitude during this time period [4]. Li et al. (2018) [3] reported on an asymmetric distribution of the hydroxyl content in the M^3 that may be due to the shielding effect, shown in Figure 1. We note that M^3 does not distinguish between hydroxyl and water. However, our previous modeling efforts in Tucker et al. (2018) [2] support the absorption feature being due to surficial OH.

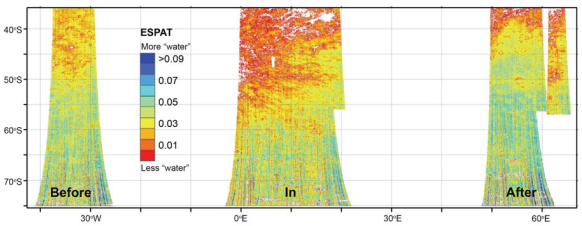

Figure 1: M^3 ESPAT values of OH content before, in and after traversing Earth's magnetotail presented in Li et al. (2018) [3].

Methodology: In this study we use a Monte Carlo model to simulate the effect of the magnetotail crossing on the surficial OH content for comparison to the M^3 observation shown in Figure 1. In addition we estimate the corresponding localized effect on the H_2 exosphere to consider the limits of its detection.

The combined diffusion and surface bound exosphere Monte Carlo model used in this study is discussed in detail in Tucker et al. (2018) [2] and references therein. The model simulates the outgassing of hydrogen atoms implanted by the solar wind by considering a distribution of activation energies values to characterize diffusion. Tucker et al. (2018) [2] found that a Gaussian activation energy distribution with peak energy U_0 = 0.5 eV and width U_W = 0.078 eV produced a diurnal modulation of surface concentrations with lower concentrations in warm regions and the highest concentrations in terminator/polar regions consistent with the Li and Milliken (2017) [1] interpretation of the M^3 spectra.

The exosphere is model simulates the ballistic trajectories H_2 tracked on a spherical grid including the lunar gravity. The model loss processes due to surface absorption, photodestruction and molecular escape. We only consider exospheric distributions produces by the thermal source H_2.

Results: In this preliminary study we included the shielding effect by turning off the solar wind source, in the model, for 8 days of the mean orbital period. As shown in Figure 2 the solar wind source is turned off when the subsolar point traverses the region labeled 'shielded surface'. This region represents a region on the near side of the Moon.

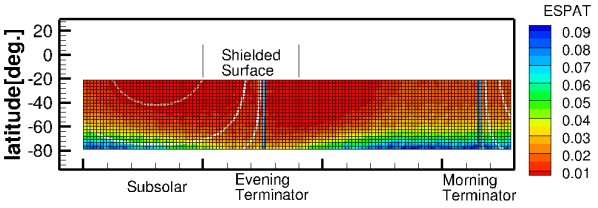

Figure 2: Model result of OH surface concentrations including shielding over 8 days of the Moon's orbit. Contour lines indicated illuminated surface with temperatures of ~120 K along terminators to 400 K at the subsolar point.

We examined the quasi steady state surface concentration including shield over the entire duration of the simulation, Figure 2. As shown in the result, we obtain an asymmetric surface concentration consistent with the ESPAT (Effective Single Particle Absorption

Thickness discussed in [1]) values for the M^3 result in Li et al. (2018) [3], shown in our Figure 1. This is the result of the decreased source of hydrogen within the 'shielded surface' regions. The M^3 ESPAT value has been shown to linear correlate with the water content (OH) in the lunar surface [3].

In Figure 3, we show the diurnal H_2 exospheric densities at 45° latitude. Typical thermally accommodated surface bound there is increase on the near surface densities over the night side. On the near side during the magnetosphere crossing we obtained a decrease in the near surface densities on by over an order of magnitude.

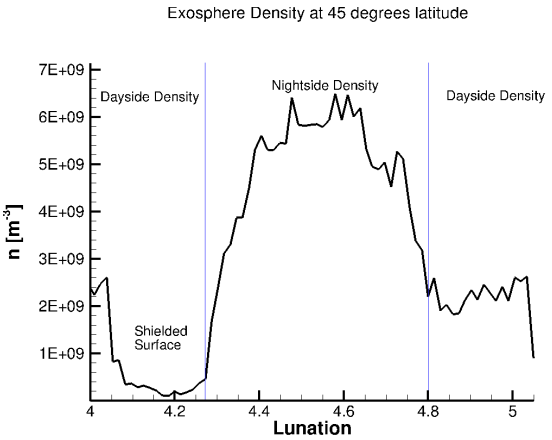

Figure 3: Model result of the near H_2 exospheric densities at 45° latitude over the lunar day.

Summary: We applied the 3D Monte Carlo model in Tucker et al. (2018) [2] to examine the effect of shielding on the OH surface concentration and H_2 exosphere. Our modeled results for the surface concentration is consistent with the M^3 ESPAT values derived for times when the Moon was shielded within Earth's magnetosphere. When turning off the solar wind source for a period of 8 days we found that the surface density of OH and near surface exospheric densities of H_2 both decreased by approximately an order of magnitude in shielded regions compared to unshielded regions. In future studies we will use more realistic plasma fluxes provided from the ARTEMIS measurements as opposed to completely turning off the source.

Acknowledgements: This work is supported by SSERVI and DREAM2.

References: [1] Li S. and Milliken R. E. (2017) *Sci. Adv.*, 3:e1701471. [2] Tucker et al. (2018) JGR, doi: 10.1029/2018JE005805, [3] Li S., Lucey, P. G., Orlando, T. M., (2018) 49th LPSC, LPI Contrib. No. 2083. [4] Poppe, A. R., Farrell, W. M., Halekas, J. S. (2017) JGR, 123.